Carbon dioxide-dependent regulation of NF- B family members RelB and p100 gives molecular insight into CO2-dependent immune regulation

Keogh, Ciara E ; Scholz, Carsten C ; Rodriguez, Javier ; Selfridge, Andrew C ; von Kriegsheim, Alexander ; Cummins, Eoin P

DOI: https://doi.org/10.1074/jbc.M116.755090

Carbon dioxide-dependent regulation of NF-κB family members RelB and p100 gives molecular insight into CO_2-dependent immune regulation

Received for publication, August 24, 2016, and in revised form, May 12, 2017 Published, Papers in Press, May 15, 2017, DOI 10.1074/jbc.M116.755090

Ciara E. Keogh[‡], Carsten C. Scholz[§¶], Javier Rodriguez[§‖], Andrew C. Selfridge[‡], Alexander von Kriegsheim[§‖], and Eoin P. Cummins[‡1]

From the [‡]School of Medicine and Conway Institute and [§]Systems Biology Ireland, University College Dublin, Dublin 4, Ireland, the [‖]Edinburgh Cancer Research Centre, Edinburgh EH4 2XR, Scotland, United Kingdom, and the [¶]Institute of Physiology, University of Zürich, CH-8057 Zürich, Switzerland

Edited by Luke O'Neill

CO_2 is a physiological gas normally produced in the body during aerobic respiration. Hypercapnia (elevated blood pCO_2 > ≈50 mm Hg) is a feature of several lung pathologies, *e.g.* chronic obstructive pulmonary disease. Hypercapnia is associated with increased susceptibility to bacterial infections and suppression of inflammatory signaling. The NF-κB pathway has been implicated in these effects; however, the molecular mechanisms underpinning cellular sensitivity of the NF-κB pathway to CO_2 are not fully elucidated. Here, we identify several novel CO_2-dependent changes in the NF-κB pathway. NF-κB family members p100 and RelB translocate to the nucleus in response to CO_2. A cohort of RelB protein-protein interactions (*e.g.* with Raf-1 and IκBα) are altered by CO_2 exposure, although others are maintained (*e.g.* with p100). RelB is processed by CO_2 in a manner dependent on a key C-terminal domain located in its transactivation domain. Loss of the RelB transactivation domain alters NF-κB-dependent transcriptional activity, and loss of p100 alters sensitivity of RelB to CO_2. Thus, we provide molecular insight into the CO_2 sensitivity of the NF-κB pathway and implicate altered RelB/p100-dependent signaling in the CO_2-dependent regulation of inflammatory signaling.

Oxygen (O_2) and carbon dioxide (CO_2) are the substrate and product of aerobic respiration, respectively. Atmospheric CO_2 levels have recently exceeded 400 ppm (0.04%) with the highest ever daily average CO_2 recorded at Mauna Loa Observatory in April, 2016 (409.44 ppm). Although the levels of this greenhouse gas are rising, the levels in the atmosphere are still much lower than that experienced within respiring organisms. CO_2 is produced as a consequence of aerobic respiration during the pre-Krebs and Krebs cycle reactions. Thus, in normocapnia the normal pCO_2 in the human circulation is ~40 mm Hg. Because the main mechanism through which CO_2 is removed from the body is via exhalation, the circulating pCO_2 is closely related to lung function and ventilation. Hyperventilation can result in lower than normal levels of CO_2 (hypocapnia), and hypoventilation and/or chronic lung diseases such as chronic obstructive pulmonary disease and cystic fibrosis result in elevated levels of CO_2 (hypercapnia) (1). In patients, the degree of hypercapnia can be profound with arterial pCO_2 values in excess of 100 mm Hg recorded in exacerbated COPD[2] (2). Hypocapnia is associated with a worse outcome in COPD (3) and worsens cerebral ischemia (4). Interestingly, hypercapnia is also associated with a worse outcome in COPD (3) with additional deleterious consequences reported in terms of muscle dysfunction (5) and immunosuppression (6). This evidence indicates that carbon dioxide is not merely a waste product of metabolism and that like oxygen it can elicit a specific repertoire of transcriptional events in a dose-dependent fashion (1, 7). In particular, genes associated with inflammation, immunity, and metabolism appear to be CO_2-sensitive and that sensitivity of these cohorts of genes to CO_2 is evolutionarily conserved (8–10). The mechanisms, however, are not well characterized. We and others have previously demonstrated sensitivity of the NF-κB pathway to CO_2 (11–16), and elevated CO_2 is associated with suppression of pro-inflammatory cytokines in a number of different settings (11, 12, 17). The current state of the art is that hypercapnia may be damaging in the context of infection (6, 18) due to immunosuppression. Conversely, hypercapnia may be of benefit in the context of destructive inflammation (19, 20) due to suppression of inflammatory signaling (1, 21). Given the importance of the NF-κB pathway in the regulation of immune and inflammatory signaling, we hypothesize that CO_2-dependent alterations in NF-κB are important in determining inflammatory signaling over a range of pCO_2 values from hypocapnia to normocapnia to hypercapnia. Our previous work has implicated members of the non-canonical NF-κB pathway (IKK, inhibitor of κB kinase (IKKα) and RelB) as being particularly sensitive to changes in CO_2 in the basal (unstimulated) state (11, 12). This study gives molec-

This work was supported by Science Foundation Ireland Grant 15/CDA/3490, University College Dublin School of Medicine, and University College Dublin Research Grant SF1146. The authors declare that they have no conflicts of interest with the contents of this article.

This article contains supplemental Figs. S1–S5 and Mass spectrometry raw data file.

[1] To whom correspondence should be addressed: School of Medicine, University College Dublin, Belfield, Dublin 4, Ireland. Tel.: 353-1-716-6317; E-mail: eoin.cummins@ucd.ie.

[2] The abbreviations used are: COPD, chronic obstructive pulmonary disease; MEF, in mouse embryonic fibroblast; IP, immunoprecipitation; F, forward; R, reverse; h, human; LFQ, label-free quantification; IKK, inhibitor of κB kinase; EMBL-EBI, European Molecular Biology Laboratory-European Bioinformatics Institute.

ular insight into CO_2-dependent modulation of the NF-κB transcription factor RelB.

NF-κB is a family of five transcription factors: p50, p65, p52, RelB, and c-Rel. Of these, p65 is the transcriptionally active component of the canonical p65-p50 heterodimer that is activated downstream of the heterotrimeric IKKα,β,γ complex (22). Oh the other hand, RelB is the transcriptionally active component of the non-canonical RelB-p52 heterodimer that is activated downstream of an IKKα homodimer complex (23). Canonical signaling is associated with the regulation of classical pro-inflammatory gene activation, *e.g.* TNFα, IL-6, and IL-1 (mainly via p65/p50 heterodimers), although non-canonical NF-κB signaling is associated with regulation of genes involved in lymphogenesis development (24, 25) (mainly via RelB/p52 heterodimers). Both canonical and non-canonical NF-κB family members demonstrate sensitivity to CO_2 in the stimulated state (11); however, non-canonical family members IKKα and RelB appear much more sensitive to CO_2 in the basal (non-ligand stimulated) state (12).

RelB is has been dubbed "an outlier in leukocyte biology" (23) and is relatively less well characterized than p65. RelB uniquely possesses an N-terminal leucine zipper domain that affects the ability of RelB to activate transcription of target genes (26); furthermore, it is postulated that RelB can activate a more diverse array of NF-κB consensus binding sequences than other family members (27). The RelB C-terminal contains a transactivation domain, which is conserved among RelA, RelB, and c-Rel (25).

Pathways regulated by RelB include those involved in the following: (i) immune development and signaling (24, 28); (ii) response to xenobiotics (29); (iii) chromatin remodeling, *e.g.* RelB can associate with the ATP-dependent SWI/SNF nucleosome-remodeling complex (30); (iv) circadian rhythms (31); and (v) cellular metabolism (23). Thus, RelB can modulate an array of cellular responses. The molecular mechanisms underpinning these effects are not yet fully appreciated. Taken together, it is clear that RelB differs significantly from other NF-κB family members in terms of structure, regulation, and target gene expression. Indeed, the relative contribution of both RelA and RelB to lymphotoxin-induced gene expression reveals both overlapping and subunit-specific target genes (32).

RelB is a labile protein subject to significant post-translational modification. Elegant biochemical studies have illustrated that RelB is a target for phosphorylation (33, 34), ubiquitination (35), sumoylation (36), signal-induced degradation, and cleavage (33, 37). These modifications regulate RelB function as well as protein-protein interactions. The protein-protein interaction between RelB and p100 is particularly important for their respective functions (34). p100 acts as an inhibitor of RelB as well as facilitating a "co-operative stabilizing state" between the two proteins (23). p100 in addition to stabilizing andinhibitingRelBhasbeenshowntoinhibitcanonicalNF-κB-dependent transcription via sequestration of RelA-p50 dimers (38). Recent work has highlighted the association of RelB (along with other NF-κB subunits) with p100 as part of a high-molecular-weight repressive "kappaBsome" (39, 40).

Finally, a recent study identified RelB mRNA expression as being associated with acid-base and cardiovascular features in patients with exacerbated COPD (41), suggesting a functional regulation of this NF-κB family member in a serious disease where hypercapnia is prevalent. The detailed mechanisms underpinning the CO_2-dependent modulation of p100 and RelB along with the downstream consequences for NF-κB-dependent signaling beyond this have not yet been elucidated and are the focus of this study.

Results

Elevated CO_2 causes a cellular re-organization of the NF-κB family members RelB and p100

We have previously reported that exposure of cells to elevated CO_2 induces RelB nuclear localization and cleavage in a number of cell types. The mechanisms underpinning this CO_2-dependent modulation of immune signaling are not fully understood and are a focus of this study. Here, we demonstrate in mouse embryonic fibroblasts (MEF) CO_2-dependent nuclear localization and cleavage of RelB that are evident over a range of CO_2 conditions (0.03, 5, and 10% CO_2) (Fig. 1, *A* and *D*). We observed a very similar pattern in lung epithelial A549 cells (supplemental Fig. S1, *A–C*). This CO_2 dose-dependent regulation of NF-κB from hypocapnia, to normocapnia, to hypercapnia highlights the importance of considering the impact of microenvironmental CO_2 concentrations in a range of conditions.

Given that RelB functionally interacts with p100 within the non-canonical NF-κB pathway, we next investigated whether p100 also demonstrated sensitivity to CO_2. Interestingly, we observed sensitivity of the p100 subunit to CO_2. To our knowledge, this is the first time that p100 sensitivity to CO_2 has been reported. p100 markedly translocates to the nucleus following exposure to 5% CO_2 and 10% CO_2 (Fig. 1, *A* and *E*). We observed a very similar pattern in lung epithelial A549 cells (supplemental Fig. S1, *A, D,* and *E*) with a more marked difference observed between 5 and 10% CO_2 in these cells. Thus, in the basal (unstimulated) state members of the non-canonical NF-κB family undergo cellular modification and re-organization by CO_2 exposure that does not appear to be a consequence of decreased pH_e, or pH_i, which remained consistent under our experimental conditions (supplemental Fig. S2).

RelB is cleaved at its C terminus in response to elevated CO_2

We next developed an overexpression system to test RelB sensitivity in HEK cells. The purpose of this was to allow us to perform mass spectrometric interactome studies in cells exposed to elevated CO_2, looking at RelB and its associated proteins (*e.g.* p100/p52). HEK cells that had been transfected with a full-length N-terminal FLAG-tagged RelB construct (Fig. 2*A*), re-capitulated the previously observed RelB response to elevated CO_2 (Fig. 1, *A* and *D*, and supplemental Fig. S1, *A–C*) (12). Interestingly, the banding pattern for RelB and FLAG from the HEK cells was almost identical (Fig. 2, *B* and *C*) suggesting that RelB is cleaved at its C terminus. Thus, we observed CO_2-dependent regulation of endogenous NF-κB family members p100 and RelB and also re-capitulated CO_2-dependent cleavage of recombinant RelB. Our next experiments were performed to gain insight into the mechanisms governing RelB sensitivity to CO_2 as well as the consequences for RelB protein-protein interactions.

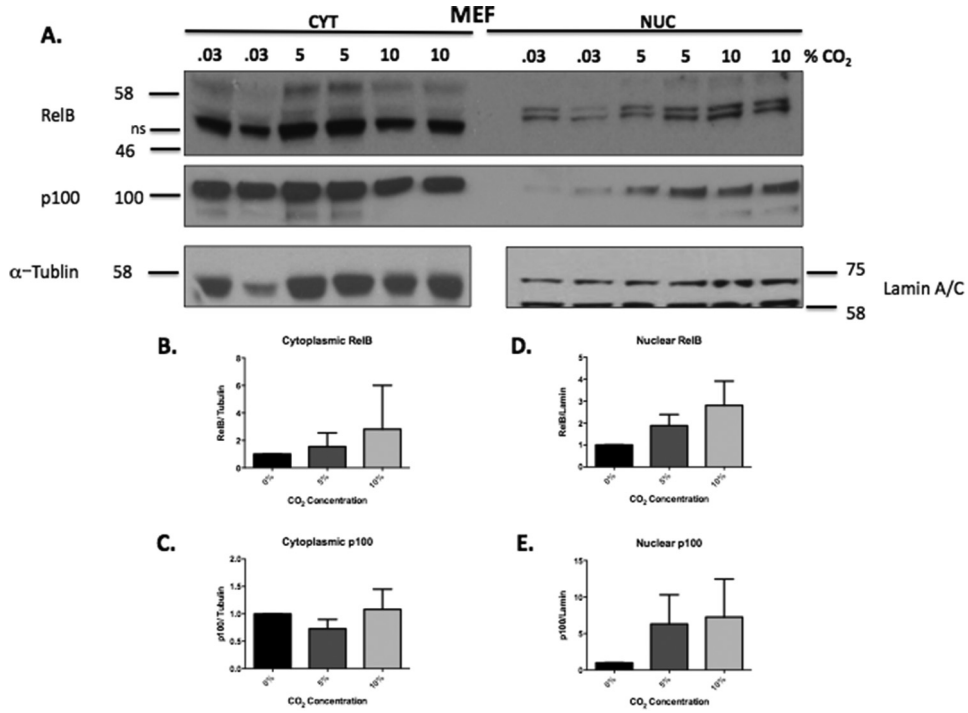

Figure 1. Elevated CO_2 causes a cellular re-organization of the NF-κB family members RelB and p100. *A,* MEF were exposed to 0.03, 5, or 10% CO_2 in pH-buffered media for 75 min prior to preparation of cytosolic (*Cyt*) and nuclear (*Nuc*) protein fractions. Lysates were immunoblotted using specific antibodies against RelB, p100/p52, lamin, and α-tubulin. *ns* denotes a nonspecific cytosolic band. *B,* densitometric quantification of cytoplasmic RelB relative to α-tubulin. *C,* densitometric quantification of cytoplasmic p100 relative to α-tubulin. *D,* densitometric quantification of nuclear RelB relative to lamin. *E,* densitometric quantification of nuclear p100 relative to lamin. Data representative of $n = 3$ experiments.

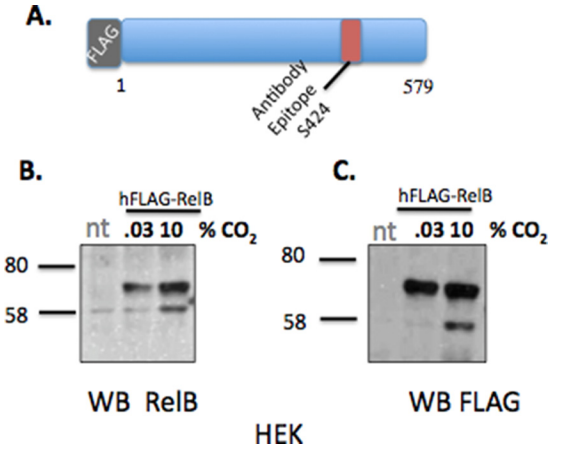

Figure 2. RelB is cleaved at its C terminus in response to elevated CO_2. *A,* schematic indicating the structure of the hFLAG-RelB construct and the region on this protein to which our RelB antibodies are directed (Ser-424). *B,* HEK cells transiently transfected with hFLAG-RelB were exposed to 0.03 or 10% CO_2 in pH-buffered media for 75 min prior to preparation of nuclear protein fractions. Lysates were immunoblotted using specific antibodies against RelB and FLAG (*C*). Data are representative of $n = >3$ experiments. *nt,* non-transfected.

RelB interactome is altered by CO_2 exposure

RelB expression and cellular localization are altered in response to CO_2 (Figs. 1, *A* and *D*, and 2, *B* and *C*, and supplemental Fig. S1, *A–C*) (12). Thus, we hypothesized that these changes were being driven at least in part by altered RelB-protein-protein interactions in the different CO_2 environments. We tested this hypothesis in an unbiased and quantitative manner. We first overexpressed FLAG-RelB in HEK cells, exposed the cells to ambient or elevated CO_2 under pH-buffered conditions, and performed an immunoprecipitation for FLAG. Precipitated proteins were then analyzed by mass spectrometry (Fig. 3*A*). Proteins of interest were then determined by meeting specific stringency thresholds for (i) enrichment over control (non FLAG-RelB-expressing cells) and (ii) evidence for CO_2 sensitivity in the RelB-specific protein interactions (2-fold difference up or down) (Fig. 3*B* and supplemental mass spectrometry files). Several known RelB-interacting proteins were identified by the screen, which supports the sensitivity of our experimental approach (Fig. 3*C*). For example, IκBα, importin α-7, and the ubiquitin C-terminal hydrolase-7 are the most enriched, the 50th most enriched, and the 90th most enriched interaction, respectively (www.ebi.ac.uk/intact). EMBL-EBI IntAct Molecular Interaction Database was searched using the search-term "RelB." Regarding CO_2 sensitivity, 25 proteins met or exceeded the thresholds for being a FLAG-RelB-associated protein that were differentially associated with RelB in a CO_2-dependent manner. These proteins are listed in supplemental Fig. S3, with a selection of proteins illustrated in Fig. 4. The seven proteins demonstrated increased association with FLAG-RelB, and 18 proteins demonstrated decreased association with FLAG-RelB at 10% CO_2 compared with ambient CO_2. Interestingly, when Gene Ontology analysis was performed on the 25 proteins that were found to have differential interactions with RelB in a CO_2-dependent manner, there was a strong enrichment of proteins involved in both protein transport and nucleic acid binding (supplemental Fig. S4). These unbiased data support the concept that RelB translocates to the nucleus in a CO_2-dependent manner, conceivably facilitated by importin proteins. Selected proteins were chosen for validation of the

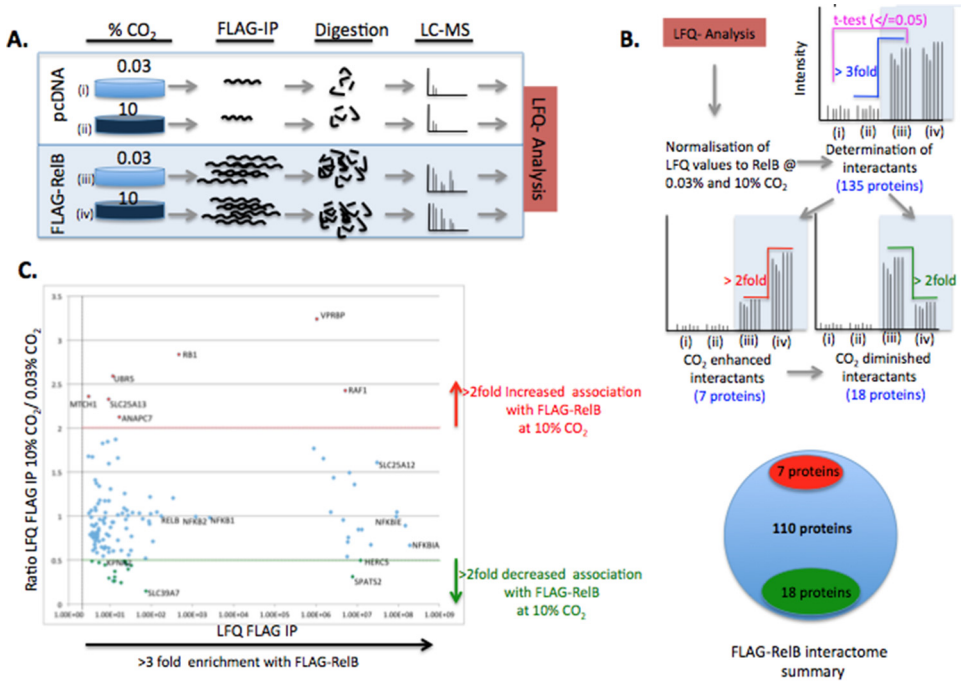

Figure 3. Mass spectrometric analysis of RelB protein-protein interactions. *A,* schematic illustrating the experimental workflow leading to the identification of proteins associated with FLAG-RelB. *B,* schematic illustrating the filtering strategy of the LFQ data to identify *bona fide* RelB interactions and RelB interactions that are altered by exposure to 10% CO_2. *C,* scatter plot of the 135 RelB protein interactions plotted for LFQ FLAG IP intensity (degree of enrichment) *versus* ratio LFQ FLAG IP 10% CO_2, 0.03% CO_2 (CO_2 sensitivity). CO_2 enhanced interactions are shown in *red*; CO_2 diminished interactions are shown in *green*, and other RelB interactions are shown in *blue*.

MS/MS screen by FLAG-RelB overexpression coupled to conventional Western blotting. RelB interactions with p100 were not affected by CO_2 exposure (supplemental Fig. S5*A*). IκBα had reduced association with RelB at 10% CO_2 in several experiments (supplemental Fig. S5), whereas Raf-1 had increased association at 10% CO_2 (supplemental Fig. S5*C*). Thus, the data from these IP Western blotting experiments support the IP MS/MS data. Of note, SMARCD2 was markedly enriched with FLAG-IP, but it was not consistently different in 10% CO_2 by IP Western blotting (supplemental Fig. S5*D*). Thus, the IP Western data largely validate the mass spectrometry data, with the MS/MS approach likely more sensitive than IP Western blotting approaches. However, given the SMARCD2 data, we suggest caution in interpreting the data from the less enriched proteins due to a risk of false positives. CO_2-dependent changes were more reproducibly validated by Western blotting for highly enriched interactors (*e.g.* IκBα, p100, and Raf-1).

Amino acids 484–503 are involved in CO_2-dependent processing of RelB

Having identified the CO_2-dependent nuclear translocation and processing of RelB (Fig. 1), we next sought to identify the region of RelB that was being cleaved. First, data from Fig. 2, *B* and *C*, suggested that RelB was being cleaved in its C-terminal region downstream of Ser-424 (the RelB antibody epitope). Second, the lower molecular weight form of RelB observed in 10% CO_2 revealed a relatively small (≈10–15 kDa) increase in electrophoretic mobility. Thus, we performed sequential mutagenesis of the C-terminal region of RelB spanning from before the RelB antibody epitope (Ser-404) (as a control) to beyond where we thought the cleavage site to likely be (Val-524). Thus, to test our hypothesis and gain molecular insight into the effects of CO_2 on RelB, we generated six mutants that individually deleted 20 amino acid segments of human RelB spanning from amino acids 404–524 (Fig. 5*A*). These mutants were screened for CO_2 sensitivity alongside a full-length RelB control. As expected, Δ404–423 (which is N-terminal to the Ser-424 RelB antibody epitope and therefore serves as an internal control) demonstrated CO_2 sensitivity analogous to that of wild-type RelB. Furthermore, this CO_2 sensitivity of Δ404–423 was blocked by pre-treatment with the proteasome inhibitor (as observed for wild-type RelB). Similarly, deletions in the regions 424–443, 444–463, and 464–483 demonstrated the same CO_2 sensitivity and MG-132 sensitivity as the wild-type FLAG-RelB construct. Interestingly, the Δ484–503 mutant did not demonstrate CO_2-dependent cleavage, whereas CO_2 and MG-132 sensitivity was restored in the downstream Δ504–524 mutant (Fig. 5*B*). Interestingly, these 20 amino acids (LLDDGFAYDPTAPTLFTMLD) reside within a highly conserved region of the protein. Taken together, these data suggest that amino acids 484–503 are within the cleavage site of RelB and/or are involved in transducing the CO_2-dependent cleavage of RelB.

RelB Δ484–579 has altered NF-κB-dependent transcriptional activity

Having identified that absence of amino acids 484–503 rendered RelB insensitive to CO_2-dependent cleavage, we hypothesized that under conditions of elevated CO_2 there is an enriched population of C-terminally truncated RelB in the nucleus. We further hypothesized that the truncated form of RelB has altered transcriptional activity and contributes to

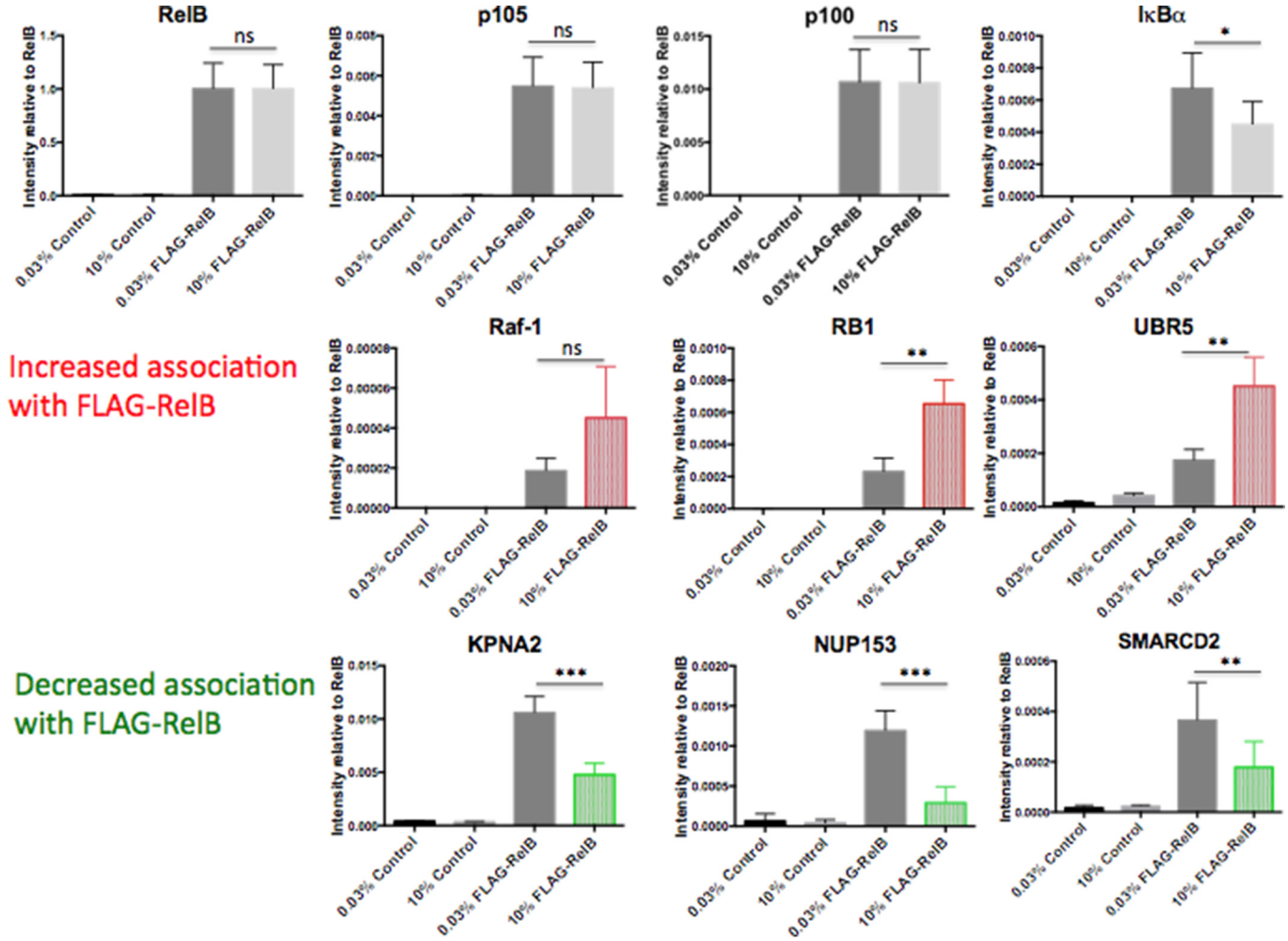

Figure 4. RelB interactome is altered by CO_2 exposure. HEK cells transiently transfected with pcDNA control plasmid or hFLAG-RelB were exposed to 0.03 or 10% CO_2 in pH-buffered media for 75 min prior to preparation of whole-cell lysates. Lysates were immunoprecipitated using FLAG-agarose, and precipitated proteins were analyzed by mass spectrometry. Data shown are protein LFQ-intensity values of selected proteins identified in the negative control and the FLAG-RelB IP at 0.03 and 10% CO_2. Selected proteins demonstrating increased association with FLAG-RelB at 10% CO_2 are highlighted in *red*, selected proteins demonstrating decreased association with FLAG-RelB at 10% CO_2 are highlighted in *green*. Data are representative of mean peptide intensity values ± S.D. relative to RelB for three biological replicates and two technical replicates per treatment. Statistical analysis comparing FLAG-RelB at 0.03 and 10% CO_2 was performed using a Student's *t* test with a *p* value ≤ 0.05 deemed significant. *ns*, not significant. *, $p \leq 0.05$; **, $p \leq 0.01$; ***, $p \leq 0.001$.

CO_2-dependent alterations in gene expression. To test the hypothesis that a truncated form of RelB has altered signaling capabilities, we generated a C-terminally truncated form of FLAG-RelB (RelB Δ484–579 also known as RelBshort (Fig. 6*A*)) and compared it with wild-type FLAG-RelB in an NF-κB-luciferase assay. TNFα-significantly increased NF-κB-luciferase activity at 0.1 and 1 ng/ml.

Overexpression of RelBshort led to reduced TNFα-stimulated NF-κB-luciferase activity compared with wild-type RelB indicating altered transcriptional activity (Fig. 6*B*). Thus, overexpression of a truncated form of RelB (that mimics the form of RelB that is enriched in the nucleus at 10% CO_2) alters cytokine-stimulated NF-κB-dependent transcriptional activity.

Loss of p100 impairs the CO_2-dependent nuclear localization of RelB

To investigate the mechanisms underpinning CO_2-dependent nuclear localization of RelB further, we focused on the interaction between p100 and RelB. p100 and RelB regulate each other's stability (34). Furthermore, p100 is known to have an inhibitory role on NF-κB signaling (38) and play a key role in the inhibitory kappaBsome (39, 40). Our earlier data demonstrated that despite a marked nuclear accumulation of RelB in response to CO_2, the interaction with p100 remained relatively constant (Figs. 3*C* and 4 and supplemental Fig. S5*A*). This suggested that p100 might also become nuclearly localized in response to elevated CO_2 and contribute to the CO_2-dependent effect on NF-κB signaling. Indeed, we observed clear p100 nuclear localization in response to elevated CO_2 (Fig. 1, *A* and *E*, and Fig. S1, *A* and *D*). These data suggest the possibility of RelB and p100 translocating to the nucleus together as part of a complex. Given the role of p100 in RelB stability (34), we hypothesized that p100 might be required to confer CO_2 sensitivity on RelB. To test this hypothesis, we compared the pattern of CO_2-dependent RelB nuclear localization in wild-type MEF and in MEF deficient in "canonical" p105 (*NFKB1*) as well as "non-

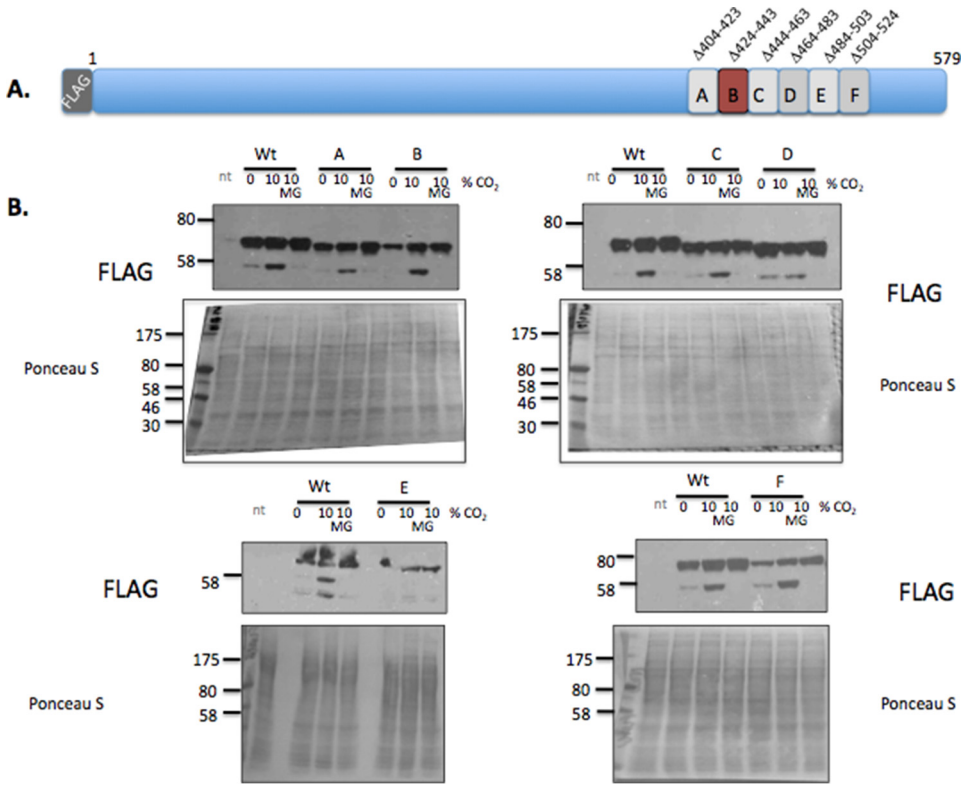

Figure 5. Amino acids 484–503 are involved in CO_2-dependent processing of RelB. *A,* HEK cells transiently transfected with full-length FLAG-RelB or one of six 20-amino acid deletions of RelB (*B*) were exposed to 0.03 or 10% CO_2 in pH-buffered media for 75 min ± Mg-132 (10 μM) prior to preparation of nuclear lysates and immunoblotting using a FLAG antibody and Ponceau S staining of the nitrocellulose membrane. Data are representative of $> n = 3$ experiments.

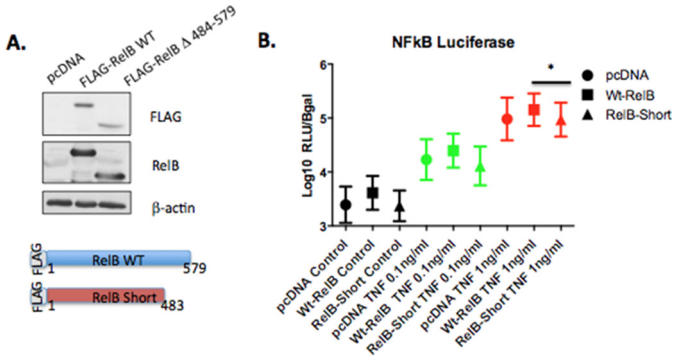

Figure 6. RelB Δ484–579 has altered NF-κB-dependent transcriptional activity. *A,* HEK cells were transiently co-transfected with pcDNA control, full-length FLAG-RelB (*WT*), or RelBshort (FLAG-RelB Δ484–579) in addition to a κB-luciferase promoter reporter construct and a β-galactosidase reporter. *B,* cells were treated with TNFα (0, 0.1, and 1 ng/ml) for 24 h at 5% CO_2. Relative light units (*RLU*) were normalized to β-galactosidase absorbance for each sample. These non-parametric data were normalized by transforming the data by log10. Data presented are mean ± S.E. for $n = 4$ experiments. Statistical analysis was performed using repeated measures one-way ANOVA, with Tukey's multiple comparisons test. A p value ≤ 0.05 was deemed significant (*, $p \leq 0.05$).

canonical" p100 (*NFKB2*). Interestingly, the $p100^{-/-}$ MEF demonstrated an aberrant pattern of nuclear RelB, compared with both the wild-type and $p105^{-/-}$ MEF. In $p100^{-/-}$ MEF, the full-length form of RelB was not enriched in the nucleus in response to elevated CO_2; however, the lower molecular weight form of RelB was observed (Fig. 7, *B*, *D,* and *F*). Taken together, this suggests that p100 NF-κB is sensitive to CO_2 and that it is required for the normal distribution of RelB in the nucleus under conditions of elevated CO_2.

Discussion

Alterations in CO_2 levels are increasingly being associated with human pathologies, *e.g.* COPD, where either hypo- or hypercapnia increases the hazard ratio for death (3). This observation is supported by *in vivo* experimentation illustrating the deleterious consequences of elevated CO_2 in the context of infection (6) and in a clinical trial where reducing hypercapnia in COPD patients was beneficial (43). Against this background, it is perhaps counterintuitive that therapeutic hypercapnia is being investigated in the context of single lung ventilation (44). There is, however, emerging evidence for elevated CO_2 being associated in a better outcome in models of inflammation (19), ventilator-induced lung injury (45, 46), skin graft survival (47), and stretch-induced epithelial injury (48). The mechanisms reconciling these seemingly opposing outcomes in hypercapnia are not fully elucidated and are a basis for this study.

Studies in both model organisms as well as human cells and tissues have implicated a role for altered NF-κB-dependent signaling in response to different CO_2 concentrations (9, 11, 12, 14, 15, 46, 49, 50). Members of the non-canonical or "alternative" NF-κB family (IKKα and RelB) have been reported to be CO_2-sensitive (11, 12), as have genes downstream of the *Drosophila* orthologue *Relish* in flies (9). Thus, we focused our attention on the transcriptionally active component of the non-canonical NF-κB pathway to gain insight into CO_2 sensing and how CO_2 affects NF-κB signaling.

Our data suggest a significant re-arrangement of RelB and p100 within the cell under conditions of elevated CO_2. Mass spectrometry analysis of immunoprecipitated RelB reveals 135

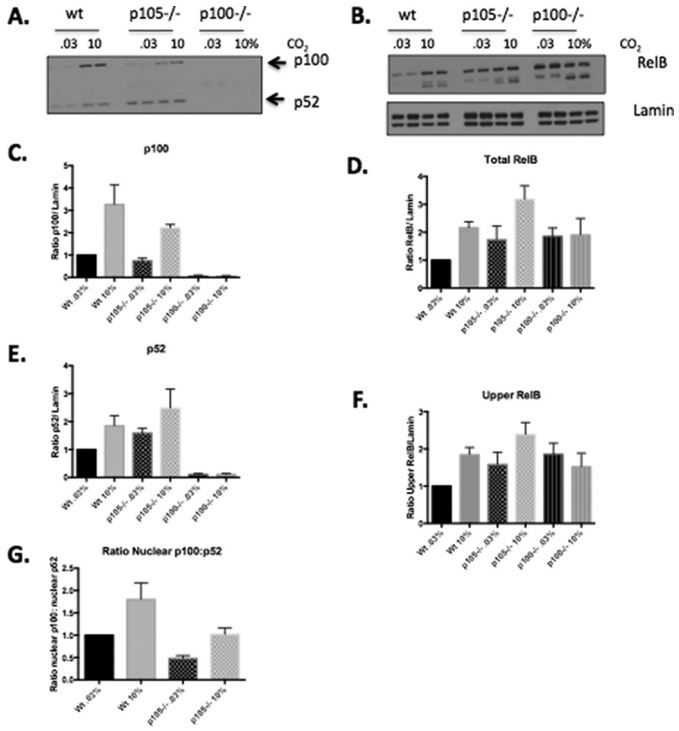

Figure 7. Loss of p100 NF-κB impairs the CO_2-dependent nuclear localization of RelB. MEF (WT *NFkB1*$^{-/-}$ (*p105*$^{-/-}$) and *NFkB2*$^{-/-}$ (*p100*$^{-/-}$)) were exposed to 0.03 or 10% CO_2 in pH-buffered media for 75 min prior to preparation of nuclear lysates. Lysates were immunoblotted using (*A*) p100/p52, (*B*) RelB and lamin-specific antibodies. Densitometric analysis was performed to determine the ratio of (*C*) p100, (*D*), total RelB, (*E*) p52, and (*F*) upper band of RelB relative to lamin. Data shown are the mean protein expression ± S.E. relative to control (WT MEF exposed to 0.03% CO_2). *G*, densitometric analysis of the ratio of nuclear p100 relative to nuclear p52 in response to elevated CO_2. Densitometric data are presented as mean ± S.E. for $n = 4$ experiments.

proteins that are 3-fold-enriched compared with control. Of these, several *bona fide* interactors (p100, IκBα, and Raf-1) were found to be significantly enriched by mass spectrometry and separately validated by conventional immunoprecipitation coupled to Western blots. Approximately 19% of these proteins were differentially associated with RelB in a CO_2-dependent manner. Thus, most RelB interactions were not significantly changed by CO_2. This is an interesting observation given that we can clearly observe marked nuclear translocation of RelB in response to elevated CO_2. This suggests that a subpopulation of RelB is actually moving into the nucleus in response to CO_2 and/or that when RelB moves into the nucleus, it does so as a complex with a number of other proteins, including p100, for example. This proposed scenario might also explain why the ratio of RelB/p100 is unchanged by CO_2. What is clear from the mass spectrometry experiment is that there is a difference in the degree of RelB interaction with proteins associated with the nucleus regarding nuclear shuttling (importins), nuclear pore, and DNA binding, for example (SMARCD2 and RB1), upon exposure to CO_2. RelB has previously been shown to have a physical association with members of the KPNA family (51). Our observed decrease in association between RelB and α-importin proteins suggests the possibility that RelB is associated with the importin α complex in advance of a stimulus, and following CO_2 exposure this interaction is reduced, as a subpopulation of RelB translocates to the nucleus. Taken together, these data point to a selective re-arrangement of RelB with its interacting partners in response to CO_2, which facilitates localization to the nucleus and may interfere with existing RelB-DNA-binding complexes.

RelB is subject to multiple post-translational modifications as well as cleavage by a variety of enzymes (33, 52, 53). Our data indicate that RelB is cleaved at its C terminus (Fig. 2, *B* and *C*). Scanning mutagenesis was employed to determine the precise site involved, to gain insight into how CO_2 modulates NF-κB-dependent signaling. Here, we report that a Δ484–503 deletion mutant of RelB demonstrates aberrant CO_2-dependent processing (Fig. 5*B*). The 484–503 region is C-terminal to the RelB nuclear localization motif, which explains why both full-length and truncated forms of RelB can accumulate in the nucleus in a CO_2-dependent manner. Furthermore, this site is distinct from other sites that have previously been reported to control RelB processing, for example Asp-205 (54), Thr-84/Ser-552 (53), and Arg-85 (52). Thus, we propose that this 20-amino acid CO_2-responsive domain of RelB is involved in CO_2-dependent cleavage of RelB. The crystal structure for this region of the RelB protein has not yet been solved, and *in silico* structural predictions of this region are of low confidence. However, region 484–503 does lie within the C-terminal transactivation domain of RelB (55). This suggests that RelB proteins deficient in the region C-terminal to the cleavage site may have impaired transcriptional activity. Previous studies have demonstrated the requirement of both N- and C-terminal regions of RelB in the presence of p50-NF-κB for full transactivation (26).

Thus, our data suggest that under conditions of elevated CO_2 RelB is cleaved and that both full-length and truncated forms of RelB can then translocate to the nucleus. It is unlikely that both of these forms of RelB have identical transcriptional activity, and consequently, we generated a RelBshort construct to test this. This truncated form of RelB (which mimics a form of RelB generated in hypercapnia) has impaired NF-κB-dependent transcriptional activity compared with full-length RelB (Fig. 6*B*).

Finally, given the known reciprocal role of p100 in stabilizing RelB, we demonstrated for the first time a profound nuclear localization of p100 in response to elevated CO_2 (Figs. 1 and 7, *A* and *C*, and supplemental Fig. S1, *A* and *D*). This is consistent with our mass spectrometry data indicating that the ratio of RelB/p100 is unchanged at 10% CO_2 and that the two proteins may translocate to the nucleus as a complex. Thus, using MEF deficient in p100, we investigated the requirement of p100 on the RelB response to elevated CO_2. Interestingly, loss of p100 significantly altered the CO_2-dependent nuclear localization profile of RelB in the nucleus (Fig. 7, *B* and *D*). Notably, a lower molecular weight form of RelB was still evident in the nucleus in response to CO_2 in p100$^{-/-}$ MEF. However, the full-length form of RelB that normally accumulates under those conditions did not (Fig. 7, *B* and *F*). Together, this suggests that p100 is important in the regulation of the RelB response to elevated CO_2 but is dispensable for the cleavage. Thus, nuclear p100 localization appears to be a key event in coordinating the NF-κB-dependent response to elevated CO_2. Interestingly, although we observed both p100 and p52 translocation to the

nucleus in response to CO_2, they did not accumulate to the same extent, with p100 relatively more enriched in the nucleus at 10% CO_2 compared with p52 (Fig. 7*G* and supplemental Fig. S1*F*). This observation first suggests that elevated CO_2 is not driving the non-canonical processing of p100 to p52 and second that a repressive p100- and RelB- containing complex is enriched in response to CO_2.

In summary, hypercapnia is a feature of a number of pathologies and is known to modulate innate and immune signaling. A role for the NF-κB pathway downstream of hypercapnia has been proposed; however, the mechanisms are not fully elucidated. Targeting CO_2-dependent signaling may represent a new anti-inflammatory strategy in the treatment of human disease; however, the molecular mechanisms downstream of CO_2 need to be more fully described. Recently, RelB has been proposed as a potential novel marker of health outcomes in exacerbated COPD (57), a condition linked to hypercapnia. Here, we show that RelB is a CO_2-sensitive transcription factor that undergoes a complex cellular rearrangement under conditions of elevated CO_2. RelB demonstrates decreased association with importin proteins, CO_2-dependent cleavage at its C-terminal that requires amino acids 484–503, and translocates to the nucleus both as a full-length protein and as a cleaved short form. RelBshort (a truncated form of RelB) demonstrates decreased NF-κB-dependent transcriptional activity compared with wild type, which may be due to impairment of its transactivation domain and consequent ability to bind nuclear proteins. The RelB interactome is altered in response to CO_2, but several RelB-protein interactions are maintained at 10% CO_2, *e.g.* interactions with p100. p100, like RelB, also translocates to the nucleus under conditions of elevated CO_2, and loss of p100 impairs RelB nuclear localization when CO_2 levels are elevated. Interestingly, in a recent cohort study of patients requiring acute mechanical ventilation, $PaCO_2$ was an independent predictor of survival to hospital discharge over a linear range of $PaCO_2$ pressures from hypocapnia (<35 mm Hg) to hypercapnia (66–75 mm Hg) (42). Thus, a better understanding of the molecular mechanisms underpinning CO_2-dependent NF-κB regulation will enhance our understanding of human pathologies where hypercapnia is a feature and help to develop CO_2-dependent therapeutic strategies.

Materials and methods

Cell culture and exposure to different CO_2 environments

Human embryonic kidney, mouse embryonic fibroblast, and A549 cells were cultured at ambient O_2 and 5% CO_2 and maintained in a humidified tissue culture incubator prior to exposure to the conditions indicated in the individual experiments.

Temperature was maintained at 37 °C in a humidified environment. CO_2 incubation was achieved by exposure of cells to preconditioned medium in an environmental chamber (COY Laboratories) set at 5 or 10% CO_2 with a balance of air. Ambient CO_2 experiments were carried out in a 37 °C humidified incubator with room air.

For experiments involving exposure to 0.03, 5, and 10% CO_2, pH buffering was achieved by supplementing high glucose DMEM powder (D1152 Sigma) with different amounts of $NaHCO_3$ as described previously (12). Media were then reconstituted, filter-sterilized, and supplemented with FCS (10%) and penicillin/streptomycin. NaCl was supplemented to correct for osmolality differences. Taken together, this approach can maintain pH_e over a range of CO_2 concentrations (0.03–10%).

Western blot analysis

Nuclear, cytosolic, whole-cell, or immunoprecipitated lysates were separated by SDS-PAGE, transferred to nitrocellulose membranes, and immunoblotted as described previously (11). Primary antibodies against RelB (4954) (Figs. 1, 6, and 7), RelB (4922) (supplemental Fig. S1), p100 (4882), and lamin (4777) (Cell Signaling Technology), α-tubulin (sc-8035) (Santa Cruz Biotechnology), and FLAG (F7425) and β-actin (A5316) (Sigma) were used, as well as species-specific HRP-conjugated secondary antibodies.

Molecular cloning/mutagenesis

hFLAG-RelB in a pCR3 (Invitrogen) backbone underwent site-directed mutagenesis of its C-terminal region using QuikChange XL mutagenesis kit according to the manufacturer's instructions. The QuikChange primer design tool was used to generate a series of deletion mutants using the following specific primers: mutant Δ404–423 F, 5′-ctcgcgaccatgacagctctgaccccca-3′, and Δ404–423 R, 5′-tgggggtcagagctgtcatggtcgcgag-3′; B mutant Δ424–443 F, 5′-cttggggagctgaaccacttcctgcccaac-3′, and Δ424–443 R, 5′-gttgggcaggaagtggttcagctccccaag-3′; C mutant Δ444–463 F, 5′-ccggccatcctggaccctgacttcttctct-3′, and Δ444–463 R, 5′-agagaagaagtcagggtccaggatggccgg-3′; mutant Δ464–483 F, 5′-ccctgctgccagacctcctggacgatgg-3′, and Δ464–483 R, 5′-ccatcgtccaggaggtctggcagcaggg-3′; mutant Δ484–503 F, 5′-gcgggcctgacctgctgccccc-3′, and Δ484–503 R, 5′-gggggcagcaggtcaggcccgc-3′; F mutant Δ504–523 F, 5′-ttcaccatgctggacgtggttggggagacc-3′, and Δ504–523 R, 5′-ggtctccccaaccacgtccagcatggtgaa-3′; and RelBshort Δ484–579 F, 5′-ccctggcgggcctgactagaagcttgaattctg-3′, and Δ484–579 R, 5′-cagaattcaagcttctagtcaggcccgccaggg-3′. Mutations were confirmed by sequencing using forward T7 and/or pCR3.1-BGHrev primers.

Transfection

Cells were transfected using plasmid DNA, OptiMEM1 serum-free media (Gibco), and Lipofectamine 2000 (Invitrogen) according to the manufacturer's instructions in antibiotic-free media. Plasmids for RelB and RelB mutants are described above.

Immunoprecipitation

HEK cells overexpressing recombinant FLAG-tagged proteins were lysed in whole-cell lysis buffer (1% Triton X-100, 20 mM Tris-HCl (pH 7.5), 150 mM NaCl, 1 mM $MgCl_2$) and incubated with anti-FLAG M2 affinity gel (7.5–15 μl/Eppendorf) end-over-end with rotation at 4 °C for 1–2 h. Samples were centrifuged at 500 rpm for 1 min to pellet the beads, which were then washed two times in lysis buffer and two times in wash buffer (lysis buffer without Triton X-100) with centrifugation in between each wash step. Beads were then incubated with

NuPAGE sample buffer (≈30–60 μl) and boiled for 5 min. The supernatant was collected, supplemented with 100 mM DTT, and boiled for a further 5 min. Samples were then frozen at −20 °C or immediately run on a Western blot.

Mass spectrometry

Following immunoprecipitation, samples were treated as followed for MS analysis. After washing twice with 300 μl of ice-cold PBS, beads with bound proteins were eluted in two steps. First, 60 μl of eluting buffer I (50 mM Tris-HCl (pH 7.5), 2 M urea, and 50 μg/ml trypsin (modified sequencing grade trypsin); Promega) were incubated while shaking at 27 °C for 30 min, and second, 25 μl of elution buffer II (50 mM Tris-HCl (pH 7.5), 2 M urea, and 1 mM DTT) was added twice. Both supernatants were combined and incubated overnight at room temperature. Samples were alkylated (20 μl of iodoacetamide, 5 mg/ml, 30 min in the dark). Then, the reaction was stopped with 1 μl of 100% trifluoroacetic acid (TFA), and 100 μl of the sample was immediately loaded into equilibrated hand-made C18 StageTips containing Octadecyl C18 disks (Supelco). Samples were desalted by using two times 50 μl of 0.1% TFA and eluted with two times 25 μl of 50% acetonitrile and 0.1% TFA solution. Final eluates were combined and concentrated until the volume was reduced to 5 μl, using a CentriVap concentrator (Labconco). Samples were diluted to obtain a final volume of 12 μl by adding 0.1% TFA. The samples were run on a Q-Exactive mass spectrometer (Thermo Fisher Scientific) connected to a Dionex Ultimate 3000 (RSLCnano) chromatography system (Thermo Fisher Scientific). Each sample was loaded onto Biobasic Picotip Emitter (120 mm length, 75 μm internal diameter) packed with Reprocil Pur C18 (1.9 μm) reverse phase media column and was separated by an increasing acetonitrile gradient, using a 53-min reverse phase gradient at a flow rate of 250 nl/min. The mass spectrometer was operated in positive ion mode with a capillary temperature of 220 °C and a capillary voltage of 1,900 V applied to the capillary. All data were acquired with the mass spectrometer operating in automatic data-dependent switching mode. A high-resolution-MS scan (350–2,000 Da) was performed using the Orbitrap to select the 12 most intense ions before MS/MS analysis using the ion trap. Raw files were analyzed, and relative protein concentration and identifications were determined by label-free quantification using the MaxQuant software suite (9). MS/MS spectra were searched against the human UniProt database. Triplicate biological samples for each treatment were performed in each case. Each individual biological sample was then run in duplicate on the mass spectrometer. Each of the triplicate biological samples was considered as an individual *n*-number for the purposes of this experiment and to determine statistical significance. We have used a similar approach previously (56).

Filtering of mass spectrometry/mass spectrometry data

Protein mass spectrometry label-free quantification (LFQ) intensity values were normalized in each replicate for the respective experimental treatments. To discriminate specific FLAG-RelB-associated interactions from nonspecific FLAG-agarose interactions, we defined several inclusion criteria.

Enriched interactions—Proteins that were enriched >3-fold in the 0.03% CO_2 and 10% CO_2 FLAG-RelB sample were compared with their respective pcDNA control sample at 0.03 and 10% CO_2 with a p value of ≤0.05 in each case. 135 proteins were enriched with FLAG-RelB using this analysis.

CO_2-sensitive interactions—Proteins that were enriched as under "Enriched interactions" above were additionally filtered for CO_2 sensitivity (ratio FLAG-RelB 10% CO_2/FLAG-RelB 0.03% CO_2, >2 or <0.05) (2-fold difference up or down). 25 proteins had a CO_2-sensitive interaction with FLAG-RelB using this analysis.

Pathway analysis of mass spectrometry/mass spectrometry data

25 CO_2-sensitive protein interactions (see under "CO_2-sensitive interactions" above for filtering of mass spectrometry data and supplemental Fig. S1) were analyzed for protein class using Panther bioinformatic software (www.pantherdb.org)[3] (58).

Densitometry

Densitometric analysis was carried out using ImageJ software to determine band size/intensity of target proteins on Western blottings and normalized to respective controls, *e.g.* α-tubulin, lamin A/C, or FLAG.

Luciferase assay

HEK cells were seeded on 24-well plates (50,000 cells/well). 24 h later, cells were co-transfected with NFκB-Luc PEST (Promega) and β-galactosidase control plasmid along with pcDNA or WT hFLAG-RelB or FLAG-RelBshort mutant RelB. 24 h later cells were treated ±TNFα (0.1–1 ng/ml) (Sigma) for 24 h prior to lysis. Lysate was incubated with luciferase substrate (Promega), and chemiluminescence was detected on a BIOTEK Synergy-HT plate reader.

pH_i assay

This experiment was performed as described previously (11). Briefly, cells were washed in OptiMEM1 (Gibco) serum-free media and loaded with 5 μM 2′,7′-bis-(2-carboxyethyl)-5-(and -6)-carboxyfluorescein, acetoxymethyl ester (BCECF-AM) (Molecular Probes Code B1170) in OptiMEM1 for 30 min at 37 °C, 21% O_2, 5% CO_2. Dye was removed, and cells were incubated in full DMEM for 30 min at 37 °C, 21% O_2, 5% CO_2. Cells were then exposed to pre-equilibrated buffered media at 0.03% CO_2, 5 or 10% CO_2 for 75 min. Following exposure, cells were removed and immediately assayed in a fluorescent plate reader at room temperature at 21% O_2, ambient CO_2. The fluorophore was excited at 485 nm (λ1) and 444 nm (λ2), and emission was recorded at 538 nm in each case. The ratio λ1/λ2 is directly proportional to intracellular pH, which was confirmed using a standard curve of nigericin (Sigma)-permeabilized cells exposed to a high potassium buffer (KCl (140 mM), $MgCl_2$ (1 mM), $CaCl_2$ (2 mM), D-glucose (5 mM)) adjusted to a range of pH values (pH 5–8) using MES (20 mM)-acidifying solution or Tris base (20 mM) alkaline solution.

[3] Please note that the JBC is not responsible for the long-term archiving and maintenance of this site or any other third party hosted site.

Author contributions—C. E. K., C. C. S., J. R., A. C. S., A. von K., and E. P. C. designed, performed, and analyzed experiments. E. P. C. conceived and coordinated the study and wrote the paper. All authors reviewed the results and approved the manuscript.

Acknowledgments—We thank Dr. Margot Thome (University of Lausanne) for the generous gift of hFLAG-RelB and Prof. Alex Hoffmann (UCLA) for generously providing the wild-type, RelB$^{-/-}$, p100$^{-/-}$, and p105$^{-/-}$ MEF.

References

1. Cummins, E. P., Selfridge, A. C., Sporn, P. H., Sznajder, J. I., and Taylor, C. T. (2014) Carbon dioxide-sensing in organisms and its implications for human disease. *Cell. Mol. Life Sci.* **71,** 831–845
2. Crummy, F., Buchan, C., Miller, B., Toghill, J., and Naughton, M. T. (2007) The use of noninvasive mechanical ventilation in COPD with severe hypercapnic acidosis. *Respir. Med.* **101,** 53–61
3. Ahmadi, Z., Bornefalk-Hermansson, A., Franklin, K. A., Midgren, B., and Ekström,M.P.(2014)Hypo-andhypercapniapredictmortalityinoxygen-dependent chronic obstructive pulmonary disease: a population-based prospective study. *Respir. Res.* **15,** 30
4. Roberts, B. W., Karagiannis, P., Coletta, M., Kilgannon, J. H., Chansky, M. E., and Trzeciak, S. (2015) Effects of PaCO2 derangements on clinical outcomes after cerebral injury: a systematic review. *Resuscitation* **91,** 32–41
5. Jaitovich, A., Angulo, M., Lecuona, E., Dada, L. A., Welch, L. C., Cheng, Y., Gusarova, G., Ceco, E., Liu, C., Shigemura, M., Barreiro, E., Patterson, C., Nader, G. A., and Sznajder, J. I. (2015) High CO2 levels cause skeletal muscle atrophy via AMPK, FoxO3a and muscle-specific ring finger protein1 (MuRF1). *J. Biol. Chem.* **290,** 9183–9194
6. Gates, K. L., Howell, H. A., Nair, A., Vohwinkel, C. U., Welch, L. C., Beitel, G. J., Hauser, A. R., Sznajder, J. I., and Sporn, P. H. (2013) Hypercapnia impairs lung neutrophil function and increases mortality in murine pseudomonas pneumonia. *Am. J. Respir. Cell Mol. Biol.* **49,** 821–828
7. Cummins, E. P., and Keogh, C. E. (2016) Respiratory gases and the regulation of transcription. *Exp. Physiol.* **101,** 986–1002
8. Sharabi, K., Hurwitz, A., Simon, A. J., Beitel, G. J., Morimoto, R. I., Rechavi, G., Sznajder, J. I., and Gruenbaum, Y. (2009) Elevated CO2 levels affect development, motility, and fertility and extend life span in *Caenorhabditis elegans*. *Proc. Natl. Acad. Sci. U.S.A.* **106,** 4024–4029
9. Helenius, I. T., Krupinski, T., Turnbull, D. W., Gruenbaum, Y., Silverman, N., Johnson, E. A., Sporn, P. H., Sznajder, J. I., and Beitel, G. J. (2009) Elevated CO2 suppresses specific *Drosophila* innate immune responses and resistance to bacterial infection. *Proc. Natl. Acad. Sci. U.S.A.* **106,** 18710–18715
10. Li, G., Zhou, D., Vicencio, A. G., Ryu, J., Xue, J., Kanaan, A., Gavrialov, O., and Haddad, G. G. (2006) Effect of carbon dioxide on neonatal mouse lung: a genomic approach. *J. Appl. Physiol.* **101,** 1556–1564
11. Cummins, E. P., Oliver, K. M., Lenihan, C. R., Fitzpatrick, S. F., Bruning, U., Scholz, C. C., Slattery, C., Leonard, M. O., McLoughlin, P., and Taylor, C. T. (2010) NF-κB links CO2 sensing to innate immunity and inflammation in mammalian cells. *J. Immunol.* **185,** 4439–4445
12. Oliver, K. M., Lenihan, C. R., Bruning, U., Cheong, A., Laffey, J. G., McLoughlin, P., Taylor, C. T., and Cummins, E. P. (2012) Hypercapnia induces cleavage and nuclear localization of RelB protein, giving insight into CO2 sensing and signaling. *J. Biol. Chem.* **287,** 14004–14011
13. Taylor, C. T., and Cummins, E. P. (2011) Regulation of gene expression by carbon dioxide. *J. Physiol.* **589,** 797–803
14. Takeshita, K., Suzuki, Y., Nishio, K., Takeuchi, O., Toda, K., Kudo, H., Miyao, N., Ishii, M., Sato, N., Naoki, K., Aoki, T., Suzuki, K., Hiraoka, R., and Yamaguchi, K. (2003) Hypercapnic acidosis attenuates endotoxin-induced nuclear factor-κB activation. *Am. J. Respir. Cell Mol. Biol.* **29,** 124–132
15. O'Toole, D., Hassett, P., Contreras, M., Higgins, B. D., McKeown, S. T., McAuley, D. F., O'Brien, T., and Laffey, J. G. (2009) Hypercapnic acidosis attenuates pulmonary epithelial wound repair by an NF-κB dependent mechanism. *Thorax* **64,** 976–982
16. Abolhassani, M., Guais, A., Chaumet-Riffaud, P., Sasco, A. J., and Schwartz, L. (2009) Carbon dioxide inhalation causes pulmonary inflammation. *Am. J. Physiol. Lung Cell. Mol. Physiol.* **296,** L657–L665
17. Wang, N., Gates, K. L., Trejo, H., Favoreto, S., Jr., Schleimer, R. P., Sznajder, J. I., Beitel, G. J., and Sporn, P. H. (2010) Elevated CO2 selectively inhibits interleukin-6 and tumor necrosis factor expression and decreases phagocytosis in the macrophage. *FASEB J.* **24,** 2178–2190
18. O'Croinin, D. F., Nichol, A. D., Hopkins, N., Boylan, J., O'Brien, S., O'Connor, C., Laffey, J. G., and McLoughlin, P. (2008) Sustained hypercapnic acidosis during pulmonary infection increases bacterial load and worsens lung injury. *Crit. Care Med.* **36,** 2128–2135
19. Laffey, J. G., Honan, D., Hopkins, N., Hyvelin, J. M., Boylan, J. F., and McLoughlin, P. (2004) Hypercapnic acidosis attenuates endotoxin-induced acute lung injury. *Am. J. Respir. Crit. Care Med.* **169,** 46–56
20. Costello, J., Higgins, B., Contreras, M., Chonghaile, M. N., Hassett, P., O'Toole, D., and Laffey, J. G. (2009) Hypercapnic acidosis attenuates shock and lung injury in early and prolonged systemic sepsis. *Crit. Care Med.* **37,** 2412–2420
21. Otulakowski, G., and Kavanagh, B. P. (2011) Hypercapnia in acute illness: sometimes good, sometimes not. *Crit. Care Med.* **39,** 1581–1582
22. Ghosh, S., and Hayden, M. S. (2012) Celebrating 25 years of NF-κB research. *Immunol. Rev.* **246,** 5–13
23. Millet, P., McCall, C., and Yoza, B. (2013) RelB: an outlier in leukocyte biology. *J. Leukocyte Biol.* **94,** 941–951
24. Yilmaz, Z. B., Weih, D. S., Sivakumar, V., and Weih, F. (2003) RelB is required for Peyer's patch development: differential regulation of p52-RelB by lymphotoxin and TNF. *EMBO J.* **22,** 121–130
25. Weih, F., Carrasco, D., Durham, S. K., Barton, D. S., Rizzo, C. A., Ryseck, R. P., Lira, S. A., and Bravo, R. (1995) Multiorgan inflammation and hematopoietic abnormalities in mice with a targeted disruption of RelB, a member of the NF-κB/Rel family. *Cell* **80,** 331–340
26. Dobrzanski, P., Ryseck, R. P., and Bravo, R. (1993) Both N- and C-terminal domains of RelB are required for full transactivation: role of the N-terminal leucine zipper-like motif. *Mol. Cell. Biol.* **13,** 1572–1582
27. Moorthy, A. K., Huang, D.-B., Wang, V. Y., Vu, D., and Ghosh, G. (2007) X-ray structure of a NF-κB p50/RelB/DNA complex reveals assembly of multiple dimers on tandem κB sites. *J. Mol. Biol.* **373,** 723–734
28. Caamaño, J., Alexander, J., Craig, L., Bravo, R., and Hunter, C. A. (1999) The NF-κB family member RelB is required for innate and adaptive immunity to *Toxoplasma gondii*. *J. Immunol.* **163,** 4453–4461
29. Baglole, C. J., Maggirwar, S. B., Gasiewicz, T. A., Thatcher, T. H., Phipps, R. P., and Sime, P. J. (2008) The aryl hydrocarbon receptor attenuates tobacco smoke-induced cyclooxygenase-2 and prostaglandin production in lung fibroblasts through regulation of the NF-κB. *J. Biol. Chem.* **283,** 28944–28957
30. Tando, T., Ishizaka, A., Watanabe, H., Ito, T., Iida, S., Haraguchi, T., Mizutani, T., Izumi, T., Isobe, T., Akiyama, T., Inoue, J., and Iba, H. (2010) Requiem protein links RelB/p52 and the Brm-type SWI/SNF complex in a noncanonical NF-κB pathway. *J. Biol. Chem.* **285,** 21951–21960
31. Bellet, M. M., Zocchi, L., and Sassone-Corsi, P. (2012) The RelB subunit of NFκB acts as a negative regulator of circadian gene expression. *Cell Cycle* **11,** 3304–3311
32. Lovas, A., Radke, D., Albrecht, D., Yilmaz, Z. B., Möller, U., Habenicht, A. J., and Weih, F. (2008) Differential RelA- and RelB-dependent gene transcription in LTβR-stimulated mouse embryonic fibroblasts. *BMC Genomics* **9,** 606
33. Neumann, M., Klar, S., Wilisch-Neumann, A., Hollenbach, E., Kavuri, S., Leverkus, M., Kandolf, R., Brunner-Weinzierl, M. C., and Klingel, K. (2011) Glycogen synthase kinase-3β is a crucial mediator of signal-induced RelB degradation. *Oncogene* **30,** 2485–2492
34. Maier, H. J., Marienfeld, R., Wirth, T., and Baumann, B. (2003) Critical role of RelB serine 368 for dimerization and p100 stabilization. *J. Biol. Chem.* **278,** 39242–39250
35. Leidner, J., Palkowitsch, L., Marienfeld, U., Fischer, D., and Marienfeld, R. (2008) Identification of lysine residues critical for the transcriptional ac-

tivity and polyubiquitination of the NF-κB family member RelB. *Biochem. J.* **416,** 117–127
36. Leidner, J., Voogdt, C., Niedenthal, R., Möller, P., Marienfeld, U., and Marienfeld, R. B. (2014) SUMOylation attenuates the transcriptional activity of the NF-κB subunit RelB. *J. Cell. Biochem.* **115,** 1430–1440
37. Hailfinger, S., Nogai, H., Pelzer, C., Jaworski, M., Cabalzar, K., Charton, J.-E., Guzzardi, M., Décaillet, C., Grau, M., Dörken, B., Lenz, P., Lenz, G., and Thome, M. (2011) Malt1-dependent RelB cleavage promotes canonical NF-κB activation in lymphocytes and lymphoma cell lines. *Proc. Natl. Acad. Sci. U.S.A.* **108,** 14596–14601
38. Basak, S., Kim, H., Kearns, J. D., Tergaonkar, V., O'Dea, E., Werner, S. L., Benedict, C. A., Ware, C. F., Ghosh, G., Verma, I. M., and Hoffmann, A. (2007) A fourth IκB protein within the NF-κB signaling module. *Cell* **128,** 369–381
39. Fusco, A. J., Mazumder, A., Wang, V. Y., Tao, Z., Ware, C., and Ghosh, G. (2016) The NF-κB subunit RelB controls p100 processing by competing with the kinases NIK and IKK1 for binding to p100. *Sci. Signal.* **9,** ra96
40. Tao, Z., Fusco, A., Huang, D. B., Gupta, K., Young Kim, D., Ware, C. F., Van Duyne, G. D., and Ghosh, G. (2014) p100/IκBδ sequesters and inhibits NF-κB through kappaBsome formation. *Proc. Natl. Acad. Sci. U.S.A.* **111,** 15946–15951
41. Labonté, L., C. P., Zago, M., Bourbeau, J., and Baglole, C. J. (2014) Alterations in the expression of the NF-κB family member RelB as a novel marker of cardiovascular outcomes during acute exacerbations of chronic obstructive pulmonary disease. *PLoS ONE* 10.1371/journal.pone.0112965
42. Fuller, B. M., Mohr, N. M., Drewry, A. M., Ferguson, I. T., Trzeciak, S., Kollef, M. H., and Roberts, B. W. (2017) Partial pressure of arterial carbon dioxide and survival to hospital discharge among patients requiring acute mechanical ventilation: A cohort study. *J. Crit. Care* **41,** 29–35
43. Köhnlein, T., Windisch, W., Köhler, D., Drabik, A., Geiseler, J., Hartl, S., Karg, O., Laier-Groeneveld, G., Nava, S., Schönhofer, B., Schucher, B., Wegscheider, K., Criée, C. P., and Welte, T. (2014) Non-invasive positive pressure ventilation for the treatment of severe stable chronic obstructive pulmonary disease: a prospective, multicentre, randomised, controlled clinical trial. *Lancet Respir. Med.* **2,** 698–705
44. Gao, W., Liu, D. D., Li, D., and Cui, G. X. (2015) Effect of therapeutic hypercapnia on inflammatory responses to one-lung ventilation in lobectomy patients. *Anesthesiology* **122,** 1235–1252
45. Otulakowski, G., Engelberts, D., Gusarova, G. A., Bhattacharya, J., Post, M., and Kavanagh, B. P. (2014) Hypercapnia attenuates ventilator-induced lung injury via a disintegrin and metalloprotease-17. *J. Physiol.* **592,** 4507–4521
46. Contreras, M., Ansari, B., Curley, G., Higgins, B. D., Hassett, P., O'Toole, D., and Laffey, J. G. (2012) Hypercapnic acidosis attenuates ventilation-induced lung injury by a nuclear factor-κB-dependent mechanism. *Crit. Care Med.* **40,** 2622–2630
47. Tzeng, Y. S., Wu, S. Y., Peng, Y. J., Cheng, C. P., Tang, S. E., Huang, K. L., and Chu, S. J. (2015) Hypercapnic acidosis prolongs survival of skin allografts. *J. Surg. Res.* **195,** 351–359
48. Horie, S., Ansari, B., Masterson, C., Devaney, J., Scully, M., O'Toole, D., and Laffey, J. G. (2016) Hypercapnic acidosis attenuates pulmonary epithelial stretch-induced injury via inhibition of the canonical NF-κB pathway. *Intensive Care Med. Exp.* **4,** 8
49. Li, A. M., Quan, Y., Guo, Y. P., Li, W. Z., and Cui, X. G. (2010) Effects of therapeutic hypercapnia on inflammation and apoptosis after hepatic ischemia-reperfusion injury in rats. *Chin. Med. J.* **123,** 2254–2258
50. Masterson, C., O'Toole, D., Leo, A., McHale, P., Horie, S., Devaney, J., and Laffey, J. G. (2016) Effects and mechanisms by which hypercapnic acidosis inhibits sepsis-induced canonical nuclear factor-κB signaling in the lung. *Crit. Care Med.* **44,** e207–e217
51. Bouwmeester, T., Bauch, A., Ruffner, H., Angrand, P.-O., Bergamini, G., Croughton, K., Cruciat, C., Eberhard, D., Gagneur, J., Ghidelli, S., Hopf, C., Huhse, B., Mangano, R., Michon, A.-M., Schirle, M., *et al.* (2004) A physical and functional map of the human TNF-α/NF-κB signal transduction pathway. *Nat. Cell Biol.* **6,** 97–105
52. Hailfinger, S., Lenz, G., Ngo, V., Posvitz-Fejfar, A., Rebeaud, F., Guzzardi, M., Penas, E. M., Dierlamm, J., Chan, W. C., Staudt, L. M., and Thome, M. (2009) Essential role of MALT1 protease activity in activated B cell-like diffuse large B-cell lymphoma. *Proc. Natl. Acad. Sci. U.S.A.* **106,** 19946–19951
53. Marienfeld, R., Berberich-Siebelt, F., Berberich, I., Denk, A., Serfling, E., and Neumann, M. (2001) Signal-specific and phosphorylation-dependent RelB degradation: a potential mechanism of NF-κB control. *Oncogene* **20,** 8142–8147
54. Kuboki, M., Ito, A., Simizu, S., and Umezawa, K. (2015) Activation of apoptosis by caspase-3-dependent specific RelB cleavage in anticancer agent-treated cancer cells: involvement of positive feedback mechanism. *Biochem. Biophys. Res. Commun.* **456,** 810–814
55. Perkins, N. D. (2007) Integrating cell-signalling pathways with NF-κB and IKK function. *Nat. Rev. Mol. Cell Biol.* **8,** 49–62
56. Rodriguez, J., Pilkington, R., Garcia Munoz, A., Nguyen, L. K., Rauch, N., Kennedy, S., Monsefi, N., Herrero, A., Taylor, C. T., and von Kriegsheim, A. (2016) Substrate-trapped interactors of PHD3 and FIH cluster in distinct signaling pathways. *Cell Rep.* **14,** 2745–2760
57. Labonté, L., Coulombe, P., Zago, M., Bourbeau, J., and Baglole, C. J. (2014) Alterations in the expression of the NF-κB family member RelB as a novel marker of cardiovascular outcomes during acute exacerbations of chronic obstructive pulmonary disease. *PLoS ONE* **9,** e112965
58. Mi, H., Muruganujan, A., and Thomas, P. D. (2013) PANTHER in 2013: modeling the evolution of gene function, and other gene attributes, in the context of phylogenetic trees. *Nucleic Acid Res.* **41,** D377–D386

Carbon dioxide-dependent regulation of NF-κB family members RelB and p100 gives molecular insight into CO_2 – dependent immune regulation.

Ciara E. Keogh[1], Carsten C. Scholz [2,4], Javier Rodriguez[2,3], Andrew C. Selfridge[1], Alexander von Kriegsheim[2,3], Eoin P. Cummins[1]

[1]School of Medicine & Conway Institute University College Dublin, [2]Systems Biology Ireland, [3] Edinburgh Cancer Research Centre, [4]Institute of Physiology, University of Zurich

Supplementary data:

Figure S1.

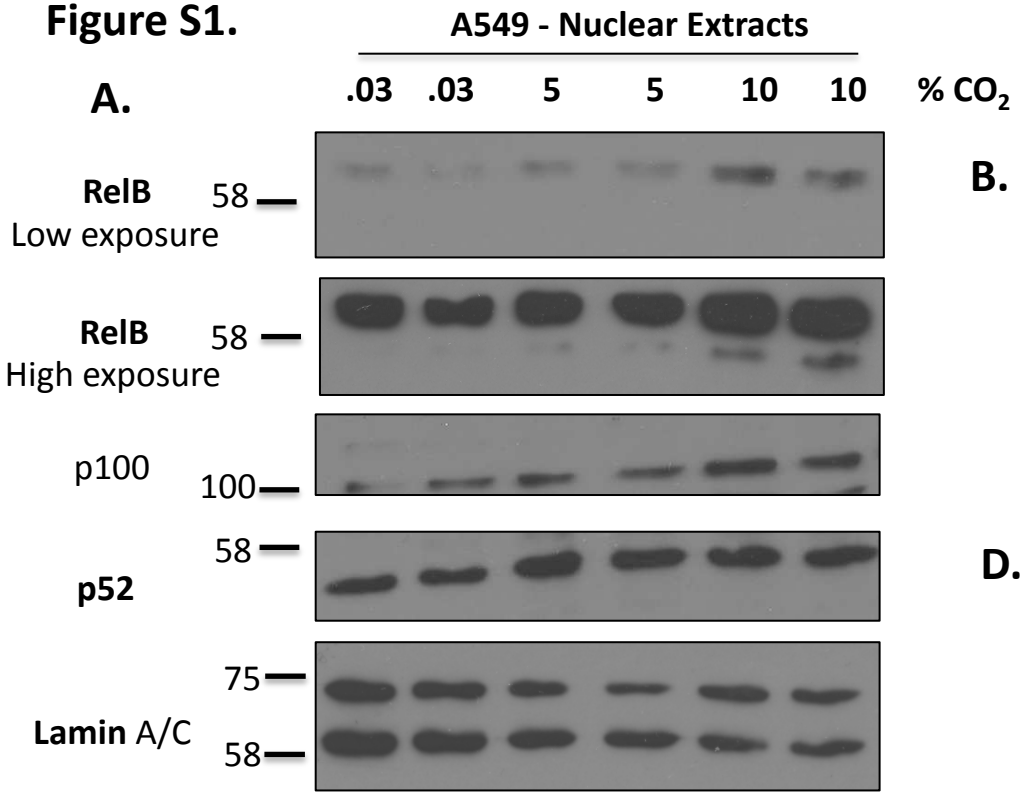

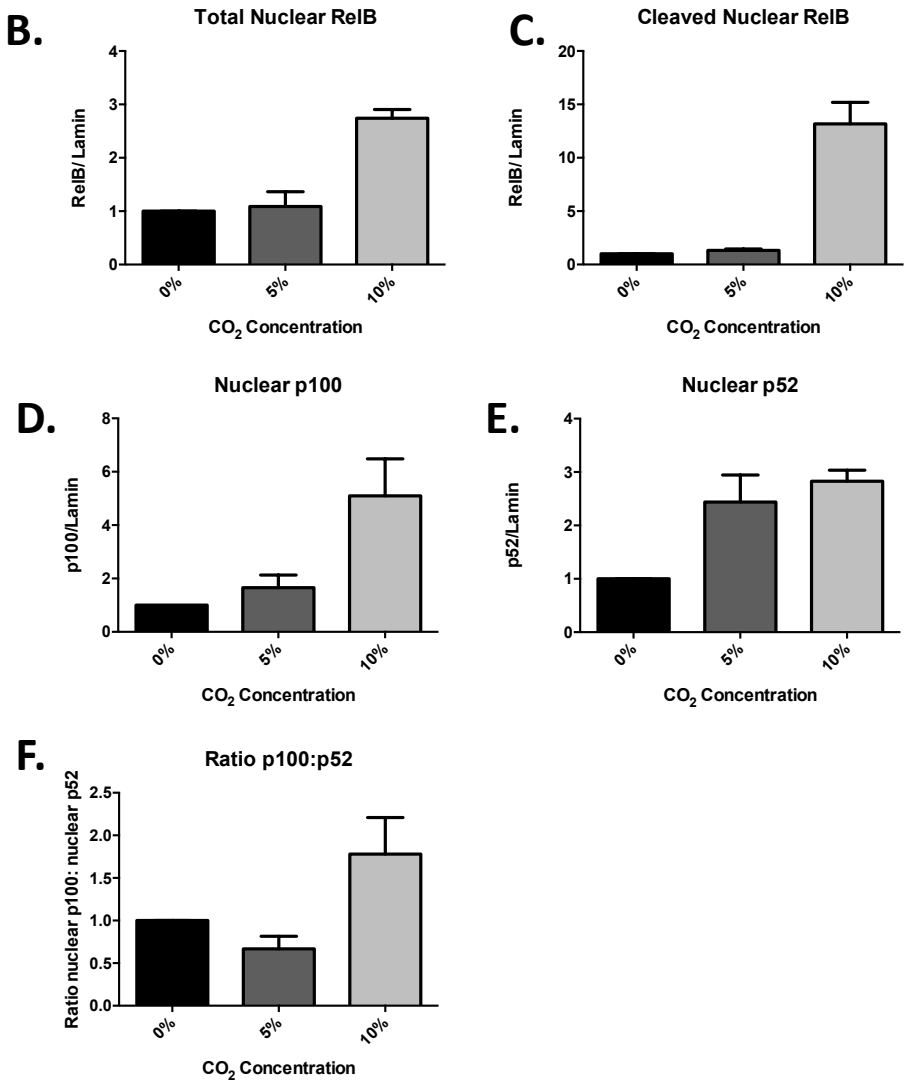

Supplementary Figure S1: (A) A549 Lung epithelial cells were exposed to 0.03, 5% or 10% CO_2 in pH buffered media for 75 mins prior to preparation of nuclear protein fractions. Lysates were immunoblotted using specific antibodies against RelB, p100/p52 and Lamin. (**B**) Densitometric quantification of nuclear RelB relative to lamin **(C.)** Densitometric quantification of cleaved nuclear RelB relative to lamin **(D)**. Densitometric quantification of nuclear p100 relative to lamin **(E)**. Densitometric quantification of nuclear p52 relative to lamin **(F)**. Ratio of nuclear p100 relative to nuclear p52 in response to elevated CO_2. Data representative of n=3 experiments.

Figure S2.

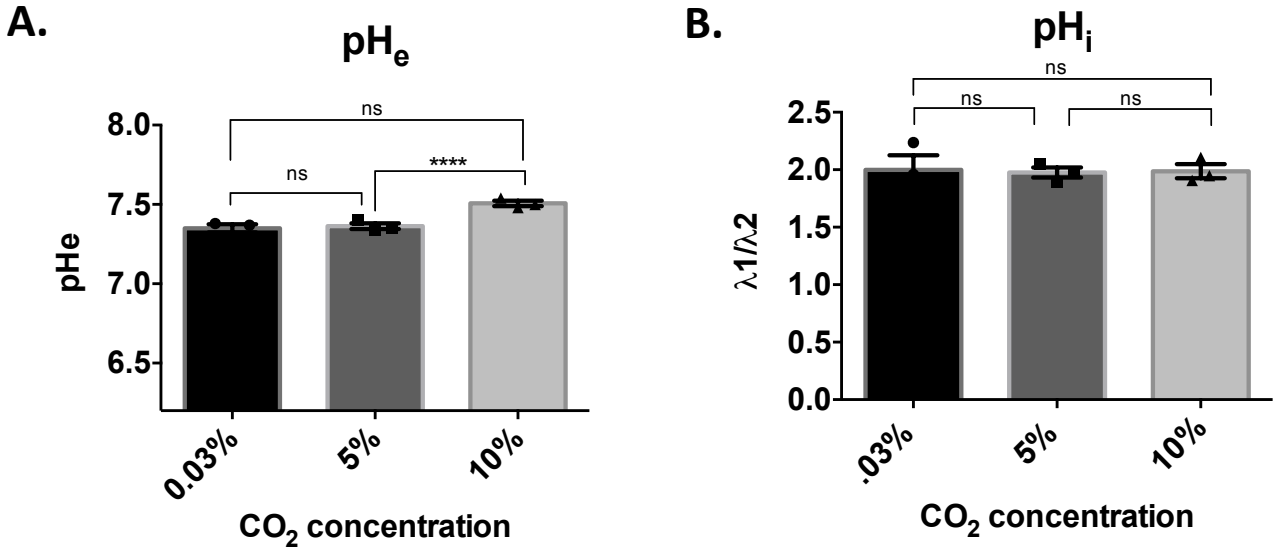

Supplementary Figure S2: (A) Extracellular pH (pH_e) values derived from bicarbonate buffered media equilibrated to 0.03%, 5% or 10% CO_2 overnight. **(B)** Intracellular pH values (pH_i) derived from MEF exposed to 0.03%, 5% or 10% CO_2 for 75 mins in bicarbonate buffered media. Values expressed are a ratio of the (λ1)/(λ2) fluorometric data using the following excitation and emission filters:
(λ1) ex485nm/em538nm
(λ2) ex444nm/em538nm
Data presented is mean +/- SEM for n=3 independent experiments. Statistical analysis was performed using a repeated measures one-way ANOVA with Tukey's post-test for multiple comparisons. p>/=0.05 deemed not significant (ns) and p</=0.001 significant (****).

Figure S3.

Protein Name	Gene Name	Ratio RelB 10%:RelB 0.03%	p-value	Significance
Zinc transporter SLC39A7	SLC39A7	0.150	0.0652	ns
Nuclear pore complex protein Nup153	NUP153;NUP153 variant protein	0.244	0.0007	***
Golgi-associated PDZ and coiled-coil motif-containing protein	GOPC	0.263	0.0032	**
Pyrroline-5-carboxylate reductase 3	PYCRL	0.264	0.0008	***
Nuclear pore complex protein Nup50	NUP50	0.297	0.0000	***
60S ribosomal protein L39;Putative 60S ribosomal protein L39-like 5	RPL39;RPL39P5	0.310	0.0001	***
Spermatogenesis-associated serine-rich protein 2	SPATS2	0.313	0.0141	*
Importin subunit alpha-3	KPNA3	0.373	0.0001	***
Aurora kinase A	AURKA	0.397	0.1674	ns
Protein transport protein Sec24B	SEC24B	0.441	0.0089	**
E3 ubiquitin-protein ligase CHIP	STUB1	0.447	0.0014	**
Importin subunit alpha-2	KPNA2	0.451	0.0001	***
	RBM6	0.467	0.0246	*
Inhibitor of nuclear factor kappa-B kinase subunit beta	IKBKB	0.471	0.0065	**
Importin subunit alpha-7	KPNA6	0.486	0.0043	**
SWI/SNF-related matrix-associated actin-dependent regulator of chromatin subfamily D member 2	SMARCD2	0.489	0.0091	**
General transcription factor 3C polypeptide 2	GTF3C2	0.489	0.0628	ns
E3 ISG15--protein ligase HERC5	HERC5	0.497	0.0189	*
Anaphase-promoting complex subunit 7	ANAPC7	2.126	0.1059	ns
Calcium-binding mitochondrial carrier protein Aralar2	SLC25A13	2.326	0.0038	**
Mitochondrial carrier homolog 1	MTCH1	2.359	0.0291	*
RAF proto-oncogene serine/threonine-protein kinase	RAF1	2.426	0.0844	ns
E3 ubiquitin-protein ligase UBR5	UBR5	2.590	0.0012	**
Retinoblastoma-associated protein	RB1	2.838	0.0024	**
Protein VPRBP	VPRBP	3.239	0.0390	*

Supplementary Figure S3. Table illustrating proteins differentially associated with FLAG-RelB in a CO_2-dependent manner. Proteins highlighted in green demonstrate decreased association with FLAG-RelB at 10% CO_2, while proteins highlighted in red demonstrate increased association with FLAG-RelB at 10% CO_2. Statistical analysis outlined in the methods.

Figure S4.

Calcium binding protein	SLC25A13				
Chaperone	STUB1				
Kinase	IKBKB	AURKA	RAF1		
Ligase	UBR5	HERC5			
Membrane traffic protein	SEC24B				
Nucleic acid binding	SMARCD2	RB1	SLC25A13	RBM6	
Transcription factor	RB1				
Transfer/carrier protein	SLC25A13	MTCH1	KPNA3	KPNA6	KPNA2
Transferase	IKBKB	AURKA	RAF1		
Transporter	SLC39A7	SLC25A13	MTCH1	NUP50	

Supplementary Figure S4. Table illustrating the results of 'protein class' analysis of 25 CO_2-dependent protein interactions with FLAG-RelB using Panther bioinformatic software.

Figure S5.

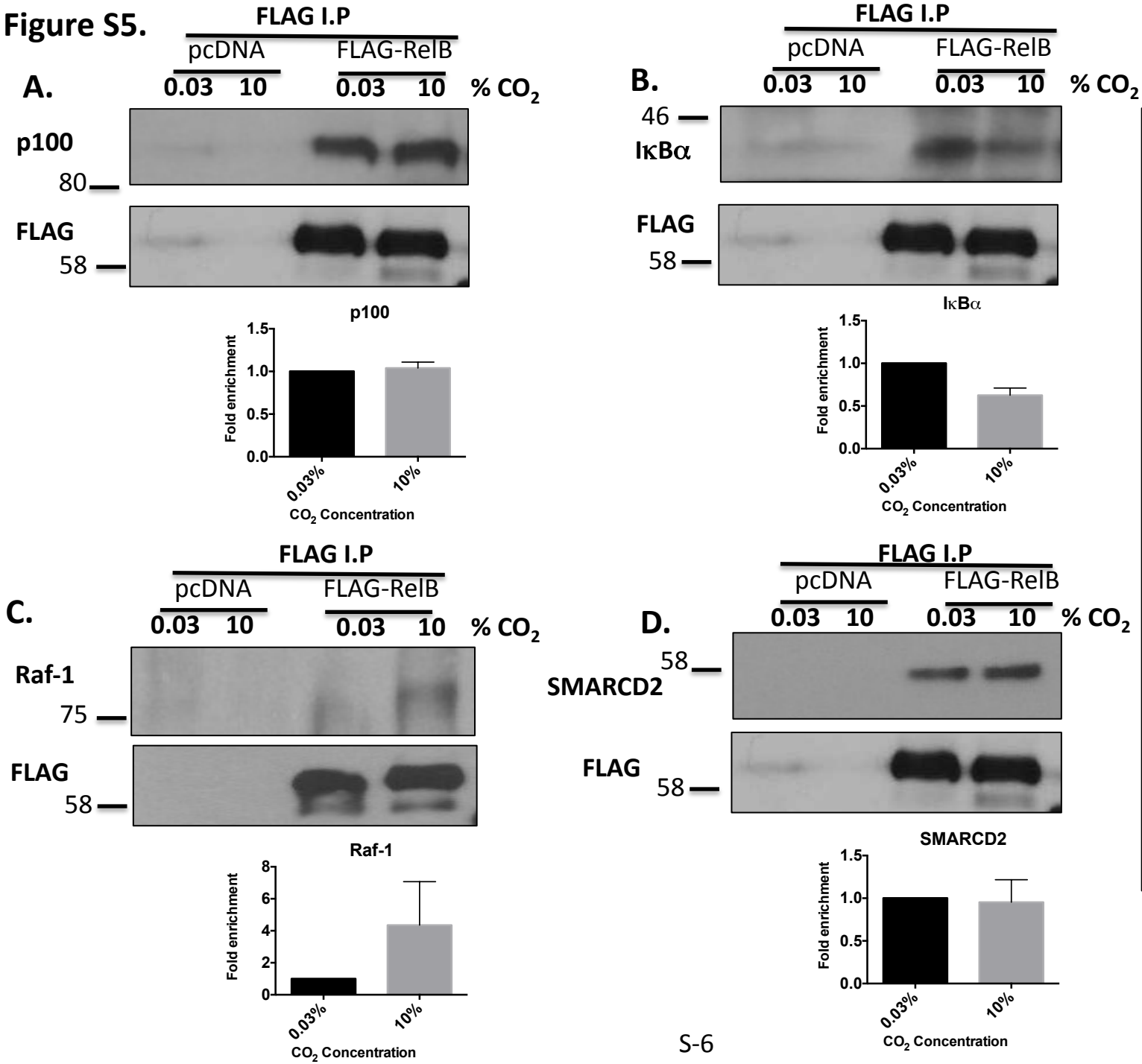

Supplementary Figure S5. HEK cells transiently transfected with pcDNA control plasmid or hFLAG-RelB were exposed to 0.03% or 10% CO_2 in pH buffered media for 75 mins prior to preparation of whole cell lysates. Lysates were immunoprecipitated using FLAG-agarose and precipitated proteins were analysed by western blot using **(A)** p100, **(B)** IκBα, **(C)** Raf-1 and **(D)** SMARCD2 antibodies. Densitometric analysis was performed for each protein and values were calculated relative to the amount of immunoprecipitated FLAG protein. Data shown is expressed as mean fold enrichment +/- SEM relative to FLAG-RelB at 0.03% CO_2 for n= 3-5 experiments.

Carbon dioxide-dependent regulation of NF-κB family members RelB and p100 gives molecular insight into CO_2-dependent immune regulation

Ciara E. Keogh, Carsten C. Scholz, Javier Rodriguez, Andrew C. Selfridge, Alexander von Kriegsheim and Eoin P. Cummins

J. Biol. Chem. 2017, 292:11561-11571.
doi: 10.1074/jbc.M116.755090 originally published online May 15, 2017